JACS
JOURNAL OF THE AMERICAN CHEMICAL SOCIETY

COMMUNICATION

pubs.acs.org/JACS

The 3D Structure of Thuricin CD, a Two-Component Bacteriocin with Cysteine Sulfur to α-Carbon Cross-links

Clarissa S. Sit,[†] Ryan T. McKay,[‡] Colin Hill,[§,∥] R. Paul Ross,[∥,#] and John C. Vederas*[,†]

[†]Department of Chemistry and [‡]National High Field NMR Centre (NANUC), University of Alberta, Edmonton, Alberta, Canada T6G 2G2

[§]Department of Microbiology and [∥]Alimentary Pharmabiotic Centre, University College, Cork, Ireland

[#]Bioscience Department, Teagasc Food Research Centre, Moorepark, Fermoy, Co. Cork, Ireland

Supporting Information

ABSTRACT: Thuricin CD is an antimicrobial factor that consists of two peptides, Trn-α and Trn-*β*, that exhibit synergistic activity against drug resistant strains of *Clostridium difficile*. Trn-α and Trn-*β* each possess three sulfur to α-carbon thioether bridges for which the stereochemistry is unknown. This report presents the three-dimensional solution structures of Trn-α and Trn-*β*. Structure calculations were performed for the eight possible stereoisomers of each peptide based on the same NMR data. The structure of the stereoisomer that best fit the experimental data was chosen as the representative structure for each peptide. It was determined that Trn-α has L-stereochemistry at Ser21 (α-R), L-stereochemistry at Thr25 (α-R), and D-stereochemistry at Thr28 (α-S) (an LLD isomer). Trn-*β* was also found to be the LLD isomer, with L-stereochemistry at Thr21 (α-R), L-stereochemistry at Ala25 (α-R), and D-stereochemistry at Tyr28 (α-S).

Bacteria can produce a wide range of antimicrobial compounds that feature structurally diverse scaffolds derived from polyketide and peptide biosynthesis. The bacteriocins, which are ribosomally synthesized antimicrobial peptides, constitute a specific class of these bacterial metabolites. Recently, we reported the isolation and characterization of thuricin CD, a two-component bacteriocin made by *Bacillus thuringiensis* DPC 6431.[1] The two components of thuricin CD, Trn-α and Trn-*β*, exhibit highly potent synergistic activity against the human pathogen *Clostridium difficile*. Structural characterization using mass spectrometry and NMR spectroscopy led to the discovery that Trn-α and Trn-*β* are posttranslationally modified: each peptide features three cysteine sulfur to α-carbon thioether bridges.

To better understand the structure and biosynthesis of these peptides, the operon for thuricin CD was fully sequenced.[1] Aside from the two structural genes for Trn-α and Trn-*β*, five other genes were uncovered. Two of these genes encode for TrnF and TrnG that together form an ATP-binding cassette (ABC) transport system used for exporting the mature peptides out of the cell. Another gene is responsible for the production of TrnE, a putative C-terminal processing peptidase that may play a role in self-immunity to thuricin CD. The remaining two genes give rise to TrnC and TrnD, both of which show sequence homology to members of the radical *S*-adenosylmethionine (SAM) superfamily of proteins.[2,3] In keeping with this homology, TrnC and TrnD each contain a cysteine-rich C-X_3-C-X_2-C motif that binds to a 4Fe-4S iron−sulfur cluster. Using SAM and the iron−sulfur clusters, TrnC and TrnD are thought to catalyze the formation of the sulfur to α-carbon bridges, potentially through a diradical mechanism.[4] As a result, the ribosomally synthesized Trn-α and Trn-*β* precursor peptides are predicted to have all L-stereochemistry but, upon posttranslational modification, could feature L- or D-stereochemistry at the α-carbons of the thioether bridges.

We now report the three-dimensional solution structures of Trn-α and Trn-*β*, determined through calculations based on multidimensional NMR studies. [^{13}C, ^{15}N]Trn-α and [^{13}C, ^{15}N]Trn-*β* were purified from the fermentation of *B. thuringiensis* in fully labeled rich media.[1] A suite of two-dimensional and three-dimensional NMR experiments was then run on each peptide. After chemical shift assignments were made for nearly every proton, carbon and nitrogen in Trn-α and Trn-*β*, structure calculations were performed using CYANA 2.1.[5] In order to determine the stereochemistry at the modified residues, the eight possible stereoisomers of each peptide were subjected to eight rounds of structure calculations using the same NMR restraints file. The resultant structures were analyzed to determine which isomer best fits the NMR data while maintaining a low root-mean-square deviation (rmsd).

Comparison of the structures generated by CYANA led to an interesting finding: for both Trn-α and Trn-*β*, the stereoisomers that matched best with the nuclear Overhauser effect (NOE) data had the same pattern of stereochemistry at the modified α-carbons. In Trn-α, the stereoisomer with L-stereochemistry at Ser21 (α-R), L-stereochemistry at Thr25 (α-R), and D-stereochemistry at Thr28 (α-S) (LLD isomer) best represented the NOE data. In Trn-*β*, the LLD isomer, with L-stereochemistry at Thr21 (α-R), L-stereochemistry at Ala25 (α-R), and D-stereochemistry at Tyr28 (α-S), also gave the best match (Figure 1).

More specifically, the LLD isomers were chosen over the other possible stereoisomers based on four criteria: greatest number of assigned NOEs used in the structure, low rmsd, low average target function value, and absence of constraint violations or Ramachandran plot irregularities. For Trn-α, the structure of the LLD isomer used 381 NOE cross-peak assignments. Only one other isomer, DLD, used the same number of assignments whereas the remaining six isomers used up to two fewer

Received: February 27, 2011
Published: April 28, 2011

dx.doi.org/10.1021/ja201802f | *J. Am. Chem. Soc.* 2011, 133, 7680–7683

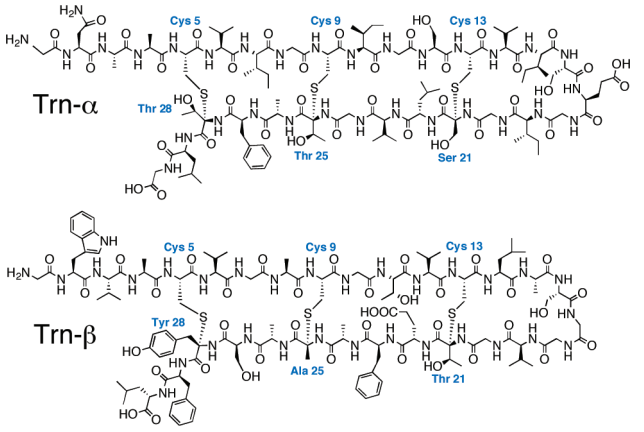

Figure 1. Chemical structures of Trn-α and Trn-*β*.

assignments. In other words, for these six isomers up to two assignments generated violations that could not be fit and were automatically discarded from the calculations by CYANA. Depending on the isomer, the assignments in question were NOEs between either a γCH_2 proton of Ile7 and the amide (HN) proton of Ala4, the HN of Gly20 and the HN of Leu22, or the Hα proton of Val23 and the Hα of Gly24. In CYANA's automated structure calculations, exclusion of these NOEs from six of the stereoisomers led to the generation of unnatural bends in the otherwise helical loops that form the two arms of the peptide. To choose between the LLD and DLD isomers, it was noted that LLD has a lower rmsd, indicating that there is less error between the 20 averaged structures generated for LLD than for DLD. As well, the LLD isomer has a lower average target function value, which serves as a measure of accuracy between the NOE restraint data entered into CYANA and the structures that are ultimately generated by the program. Finally, the overall structure of the LLD isomer gave better-formed α-helical loops than the structure of the DLD isomer.

For Trn-*β*, the structures of the LLD and LDD isomers used 313 NOE cross-peak assignments. Comparison of these structures with those of the other six isomers revealed a consistent pattern. If the stereochemistry of Thr21 were set to D instead of L, the generated structures would discard two NOEs observed between the H*β* of Thr21 and the HN of Glu22. In fact, the structure calculations for the DLL and DLD isomers generated a coupling constant violation and a distance constraint violation, respectively. If the stereochemistry of Tyr28 were set to L instead of D, a long-range NOE between the HN of Tyr28 and one of the H*β* of Cys5 would be discarded from the structure calculations. Since these NOEs involve crucial contacts to the posttranslationally modified residues, they provide strong evidence to support Thr21 having L-stereochemistry and Tyr28 having L-stereochemistry. To choose between the LLD and LDD isomers, then, it was again noted that the LLD isomer had a lower rmsd and a lower average target function value than does the LDD isomer.

Overall, the three-dimensional structures of Trn-α and Trn-*β* each consist of a helical backbone that is folded in half and held together by three sulfur to α-carbon thioether bridges (Figure 2). Coordinates for Trn-α and Trn-*β* have been deposited in the Protein Data Bank (2l9x and 2la0, respectively), and chemical shift assignments have been deposited in the BioMagResBank (17492 and 17495, respectively). To date, the only other three-dimensional structure that has been reported for a peptide

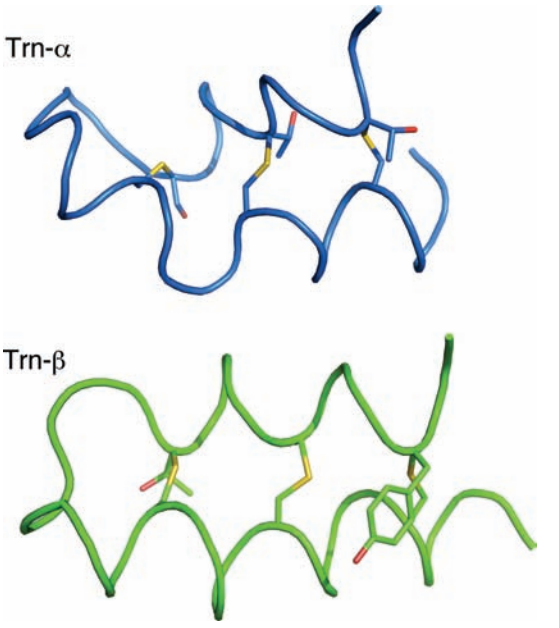

Figure 2. Cartoon representation of the three-dimensional solution structures of Trn-α (LLD isomer) and Trn-*β* (LLD isomer). In both structures, the N-terminus is closer to the lower right-hand corner of the image.

Table 1. Structural Statistics for Trn-α LLD and Trn-*β* LLD

	Trn-α LLD	Trn-β LLD
Distance and angle restraints		
total cross peak assignments	381	313
short ($\|i-j\| \leq 1$)	346	298
medium ($1 < \|i-j\| < 5$)	26	5
long ($\|i-j\| \geq 5$)	9	10
no. of ϕ angles	12	19
average target function value	0.05	0.06
rmsd (Å) for residues 1-29		
backbone	2.02 ± 0.76	1.73 ± 0.50
heavy atoms	2.50 ± 0.94	2.22 ± 0.49
rmsd (Å) for residues 5-13 & 21-28		
backbone	1.62 ± 0.71	1.14 ± 0.29
heavy atoms	2.20 ± 0.96	1.66 ± 0.29

containing sulfur to α-carbon linkages is the solution structure for subtilosin A.[4,6] Certain similarities can be found when comparing the structures of Trn-α and Trn-*β* with the structure of subtilosin A. In particular, most of the amino acid side chains in all three peptides are pointing outward, away from the center of the molecules. In addition, a high prevalence of glycine residues in each peptide affords greater flexibility, enabling the backbones to form two helical coils that are packed together in close proximity.

The structural statistics for Trn-α LLD and Trn-*β* LLD are summarized in Table 1. The backbone rmsd's for Trn-α (2.02 Å) and Trn-*β* (1.73 Å) are comparable to the backbone rmsd for subtilosin A (2.0 Å). Since most of the long-range NOEs arise from the residues that form the thioether bridges, the portions of the two peptides that are encompassed by the bridges (residues 5−13 and 21−28) are better defined and thus have lower

dx.doi.org/10.1021/ja201802f |*J. Am. Chem. Soc.* 2011, 133, 7680–7683

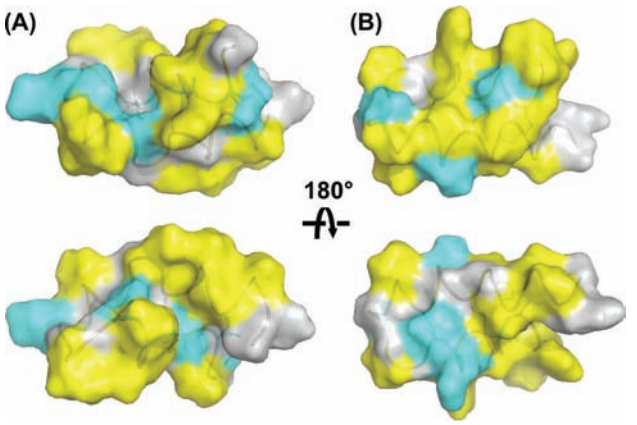

Figure 3. Surface hydrophobicity of (A) Trn-α LLD and (B) Trn-β LLD, with hydrophobic residues highlighted in yellow and hydrophilic residues highlighted in cyan. The backbone coil and sulfur to α-carbon bridges are drawn in to indicate the orientation of the peptides.

backbone rmsd's (1.62 Å for Trn-α and 1.14 Å for Trn-β). Indeed, if the backbones of the 20 lowest energy conformers for each peptide are overlaid (see Supporting Information), it can be seen that the two helical coils (residues 5−13 and 21−28) superimpose reasonably well. In contrast, the region that connects the two coils (residues 14−20) as well as the N- and C-termini have poor overlap between the 20 conformers, indicating a high degree of flexibility and freedom of movement in those segments of the peptides.

Examining the surface properties of each molecule, Trn-α has most of its hydrophilic residues bound in the thioether bridges or concentrated toward the flexible loop region (Figure 3). Trn-β, on the other hand, has its hydrophilic residues distributed over different parts of the molecule. In both cases, however, the vast majority of the peptide surface is hydrophobic as a result of having a large number of hydrophobic residues with side chains that point outward. These solution structures help explain the inherent insolubility of Trn-α and Trn-β, both of which require at least 50% organic solvent to dissolve.

The electrostatic surface potential of both peptides is largely governed by the presence of a glutamic acid residue in each sequence, as well as by the N- and C-termini. Overall, the peptides are anionic at neutral pH, with positively and negatively charged regions distributed evenly over the surfaces of the peptides (see Supporting Information).

The 3D structures presented in this report have implications for several areas of study. Due to similarities in their solution structures and the presence of the sulfur to α-carbon thioether bridges, it can be said that Trn-α and Trn-β belong to a new, emerging class of bacteriocins alongside subtilosin A.[4] Liu et al. have characterized another example of this class: a sporulation killing factor (SKF) from *Bacillus subtilis* that features a thioether bridge to the α-carbon of a methionine residue.[7] There have also been reports of other peptides with similar amino acid sequences as Trn-α and Trn-β, suggesting that numerous peptides with sulfur to α-carbon cross-links exist and that our approach could be used to elucidate the three-dimensional structures of these highly related bacteriocins.[8−13] More importantly, the solution structures of Trn-α and Trn-β may provide a starting point for the study of thuricin CD's mechanism of action. Although it has been proposed that subtilosin A and related peptides target and disrupt bacterial cell membranes, no specific receptor has been identified for these molecules.[14−17] In this regard, NMR binding studies to determine the specific target of thuricin CD and the mechanism of synergistic activity between Trn-α and Trn-β may prove to be highly interesting.

■ ASSOCIATED CONTENT

Supporting Information. Experimental procedures for NMR spectroscopy and structure calculations, experimental parameters for NMR experiments, full chemical shift assignments, ^{15}N-HSQCs, images of backbone overlay, renderings of electrostatic surface potential. This material is available free of charge via the Internet at http://pubs.acs.org.

■ AUTHOR INFORMATION

Corresponding Author
john.vederas@ualberta.ca

■ ACKNOWLEDGMENT

We thank Mark Miskolzie of the University of Alberta Chemistry Department for advice regarding NMR experiments. We thank Dr. Leah Martin-Visscher and Dr. Pascal Mercier for assistance with the CYANA software. This work was supported by the Alberta Scholarship Programs (to C.S.S.), the Natural Sciences and Engineering Research Council of Canada (NSERC), the Canada Research Chair in Bioorganic and Medicinal Chemistry, and the Alberta Heritage Foundation for Medical Research (AHFMR).

■ REFERENCES

(1) Rea, M. C.; Sit, C. S.; Clayton, E.; O'Connor, P. M.; Whittal, R. M.; Zheng, J.; Vederas, J. C.; Ross, R. P.; Hill, C. *Proc. Natl. Acad. Sci. U.S.A.* **2010**, *107*, 9352–9357.

(2) Fontecave, M.; Atta, M.; Mulliez, E. *Trends Biochem. Sci.* **2004**, *29*, 243–249.

(3) Zheng, G. L.; Yan, L. Z.; Vederas, J. C.; Zuber, P. *J. Bacteriol.* **1999**, *181*, 7346–7355.

(4) Kawulka, K. E.; Sprules, T.; Diaper, C. M.; Whittal, R. M.; McKay, R. T.; Mercier, P.; Zuber, P.; Vederas, J. C. *Biochemistry* **2004**, *43*, 3385–3395.

(5) Güntert, P.; Mumenthaler, C.; Wüthrich, K. *J. Mol. Biol.* **1997**, *273*, 283–298.

(6) Kawulka, K.; Sprules, T.; McKay, R. T.; Mercier, P.; Diaper, C. M.; Zuber, P.; Vederas, J. C. *J. Am. Chem. Soc.* **2003**, *125*, 4726–4727.

(7) Liu, W. T.; Yang, Y. L.; Xu, Y. Q.; Lamsa, A.; Haste, N. M.; Yang, J. Y.; Ng, J.; Gonzalez, D.; Ellermeier, C. D.; Straight, P. D.; Pevzner, P. A.; Pogliano, J.; Nizet, V.; Pogliano, K.; Dorrestein, P. C. *Proc. Natl. Acad. Sci. U.S.A.* **2010**, *107*, 16286–16290.

(8) Lee, H.; Churey, J. J.; Worobo, R. W. *FEMS Microbiol. Lett.* **2009**, *299*, 205–213.

(9) Sebei, S.; Zendo, T.; Boudabous, A.; Nakayama, J.; Sonomoto, K. *J. Appl. Microbiol.* **2007**, *103*, 1621–1631.

(10) Chehimi, S.; Delalande, F.; Sable, S.; Hajlaoui, A. R.; Van Dorsselaer, A.; Limam, F.; Pons, A. M. *Can. J. Microbiol.* **2007**, *53*, 284–290.

(11) Ahern, M.; Verschueren, S.; van Sinderen, D. *FEMS Microbiol. Lett.* **2003**, *220*, 127–131.

(12) Gray, E. J.; Di Falco, M.; Souleimanov, A.; Smith, D. L. *FEMS Microbiol. Lett.* **2006**, *255*, 27–32.

(13) Kamoun, F.; Mejdoub, H.; Aouissaoui, H.; Reinbolt, J.; Hammami, A.; Jaoua, S. *J. Appl. Microbiol.* **2005**, *98*, 881–888.

(14) Thennarasu, S.; Lee, D. K.; Poon, A.; Kawulka, K. E.; Vederas, J. C.; Ramamoorthy, A. *Chem. Phys. Lipids* **2005**, *137*, 38–51.

(15) Chehimi, S.; Pons, A. M.; Sable, S.; Hajlaoui, M. R.; Limam, F. *Can. J. Microbiol.* **2010**, *56*, 162–167.
(16) Huang, T.; Geng, H.; Miyyapuram, V. R.; Sit, C. S.; Vederas, J. C.; Nakano, M. M. *J. Bacteriol.* **2009**, *191*, 5690–5696.
(17) Yamamoto, K.; Xu, J. D.; Kawulka, K. E.; Vederas, J. C.; Ramamoorthy, A. *J. Am. Chem. Soc.* **2010**, *132*, 6929–6931.